Role of Phosphate Species and Speciation Kinetics in DetergencySolutions

Role of phosphate species and speciation kinetics in detergency solutions.

Giulio Isacco Lampronti[1], Gilberto Artioli[2], Liliana Oliva[3], Alessandro Ongaro[3], Stefano Maretto[3], Francesca Bonino[4,5], Katia Barbera[5], Silvia Bordiga[5]*

[1] Dipartimento di Chimica, Università di Bologna, Via Selmi 2, I-40126 Bologna, Italy

[2] Dipartimento di Geoscienze, Università di Padova, Via Gradenigo 6, I-35131 Padova, Italy

[3] Reckitt Benckiser Italia, s.p.a., Riv. Matteotti 12, I-30034 Mira, Venezia, Itay

[4] Dipartmento di Chimica IFM, Università di Torino, Via Pietro Giuria 7, I-10125 Torino, Italy

[5] NIS Centre of Excellence, Università di Torino, Via Quarello 11, I-10135 Torino, Italy

*corresponding author's email address: giulio.lampronti@unibo.it

RECEIVED DATE (to be automatically inserted after your manuscript is accepted if required according to the journal that you are submitting your paper to)

ABSTRACT

The present investigation addresses the mechanisms of inorganic phases precipitation from detergency solutions of low polyphosphate formulation. In washing machine systems the main precipitation agent is $Na_4P_2O_7 \cdot 10H_2O$ that constitutes up to 10 wt% of commercial $Na_5P_3O_{10} \cdot 5H_2O$. The solid incrustation on the heating coil is mainly formed by amorphous calcium pyrophosphate, subsequently transforming first into amorphous calcium ortophosphate and then into low crystallinity hydroxylapatite. The tripolyphosphate eventually present in the precipitates hydrolizes as well at the working temperature

present at the surface of the washing machine coil (100 °C). The pyrophosphate presence strongly inhibits the crystallization of hydroxylapatite in the washing system, thus thermal treatment of amorphous Ca-pyrophosphate is a viable mechanism to produce hydroxylapatite with controlled crystallinity. A range of analytical techniques including X-Ray diffraction, IR spectroscopy, liquid- and solid-state NMR were employed to quantify the speciation kinetics in solution, to characterize the nature of the precipitates, and to monitor the phase transformations in the solid.

KEYWORDS: phosphates, tripolyphosphates, pyrophosphate, orthophosphate, detergency, incrustation, speciation kinetics.

INTRODUCTION

Crystal Sodium tripolyphosphate ($Na_5P_3O_{10}$) is widely employed as a builder in detergency solutions, mostly to lower water hardness by complexing calcium and magnesium ions.[1] Figure 1 modified from Quimby (1954)[2] shows the tripolyphosphate (TPP) role in the phase diagram at 60 °C. The TPP concentration in a water solution for detergency with low phosphate formulation is marked in th epicture: according to the diagram there should be no precipitation under these conditions. However the water temperature is not constant during the washing cycles in laundry machines with internal heating system, and the local conditions change in time and space. Specifically the temperature may reach above 100 °C on the coil surface during the heating stage.

Apart TPP, in the real system., the industrial starting materials commonly contain a variable initial amount (5-10 wt%) of pyrophosphate due to hydrolisis reactions occurring in the slurry stage of the TPP production process.[3] Morevoer, TPP can hydrolize in the washing machine water system as well:[4]

$$P_3O_{10}^{5-} + H_2O \rightarrow P_2O_7^{4-} + PO_4^{3-} + 2H^+ \quad \text{(eq.1)},$$

thus increasing the pyrophosphate (PYP) and the orthophosphate (ORP) concentration in the detergency solution. Further, PYP can hydrolize too:

$$P_2O_7^{4-} + H_2O \rightarrow 2PO_4^{3-} + 2H^+, \quad \text{(eq.2)}$$

although the kinetics of the latter speciation (eq.2) is 1-2 orders of magnitude slower than eq.1.[5]

The ORP role in solution is known and widely studied in the literature, being the Ca form: calcium ORP's are strongly insoluble salts[6] Thus ORP acts as a precipitating agent in any possible condition of the considered system. On the other hand, the PYP plays a dual role At lower temperature, it is a complexing agent at low temperature as and even better than TPP: every g/l of sodium PYP (MW = 266) can keep in solution 650 mg/l of calcium carbonate at room temperature, while each g/l of sodium TPP (MW = 368) is able to keep in solution 320 mg of calcium carbonate.[1] At temperature higher than 40 °C PYP is a precipitating agent.[7]

When TPP is largely in excess, its chelation rate is such that the solution free water hardness decreases to extremely low values, easily lower than 10 ppm of calcium. In these conditions PYP and ORP are not a problem and their precipitation is virtually forbidden. On the contrary when TPP concentration decreases to 3 g/l or lower, as it happens in low polyphosphate formulation detergents (sodium TPP < 30 wt%), both PYP and ORP can precipitate if water hardness is higher than> 35 °F).[1]

Therefore, the quantification of all the (poly)phosphatic species concentration in the system, in the liquid and in the solid as well, in order to understand the precipitation mechanisms, is crucial and fundamental to develop appropriate precipitation inhibitors with specific properties.

The present investigation addresses the mechanisms of inorganic phases precipitation from detergency solutions of low polyphosphate formulation using a range of analytical techniques, since incrustation problems often arise during repeated detergency cycles in washing machines. The objective is to obtain

a better control of the phosphate precipitation through the full investigation of the speciation kinetics in solution, and the characterization of the nature and phase transformations in the solid precipates.

.

MATERIALS AND METHODS

All **Kinetic Experiments**

Sodium TPP ($Na_5P_3O_{10}\cdot 5H_2O$) was provided by Reckitt & Benckiser Italy and contained 5-10 wt% of sodium PYP ($Na_4P_2O_7\cdot 4H_2O$). All other chemicals were reagent grade. Static solution experiments were conducted at constant temperature, and the speciation at regular intervals measured by solution ^{31}P NMR. Samples were collected at regular time intervals, and measured quickly at room temperature. Table 1 reports the details of the experimental conditions.

Table 1: kinetic experiments labels and setting details.

Label	**T**	**pH**	**[$Na_5P_3O_{10}$]**	**[$NaHCO_3$]**
KE1	95°C	9.5	18.9 g/l	42 g/l
KE2	95°C	10.5	18.9 g/l	42 g/l
KE3	95°C	11.5	18.9 g/l	42 g/l
KE4	85°C	9.5	18.9 g/l	42 g/l
KE5	85°C	9.5	6.3 g/l	42 g/l
KE6	85°C	9.5	6.3 g/l	2.1 g/l

NMR Measurements In Solution

TPP, PYP, and ORP concentrations were measured via ^{31}P NMR spectrometry.. NMR spectra were collected at room temperature with a Bruker 400 AMX spectrometer. Molar fractions were calculated from peak areas.

Precipitation Experiments

The same TPP starting materials used for the preparation of solutions was also used to produce the solid phases. All other chemicals were reagent grade. The experiments were aimed to check the total amount of solid precipitated in different conditions, and to measure the relative proportion of the phosphate species.

Calcium (poly)phosphate precipitates were synthesized by keeping simulated detergency solutions at constant temperature and volume. Table 2 reports all performed experiments at different pH, temperature, and time. The selected solution concentrations are marked in Fig. 1. The precipitates were collected by filtering on Nuclepore polycarbonate filters (pore size 0.2 μm), washed by passing deionized water through the filter, and dried at room temperature.

Table 2: precipitation experiments labels and setting details.

Label	**Solution chemistry**	**pH**	**Temperature**	**Time**
SE1	0 °F, no other added solute	unbuffered pH	60°C	1 week
SE2	43°F , common detergency solution composition*	buffered pH = 10.50	95°C	20 h
SE3	43°F , common detergency solution composition	buffered pH = 10.50	90°C	18 h
SE4	43°F , common detergency solution composition**	buffered pH = 10.50	90°C	18 h
SE5	43°F , common detergency solution composition	buffered pH = 10.50	80°C	24 h

SE6	43°F , common detergency solution composition	buffered pH = 10.50	90°C	24 h
SE7	43°F , common detergency solution composition	buffered pH = 10.50	60°C	24 h
SE8	80°F, $CaCl_2$ only ***	unbuffered pH	25°C	30 m

*Simulated detergency solution composition: (Ca/Mg)mol = 2.58; [$CaCl_2 \cdot 2H_2O$] = 3.1 mmol/l, [$MgSO_4 \cdot 7H_2O$] = 1.2 mmol/l, Na_2SO_4 = 25 mmol/l, $NaHCO_3$ = 21 mmol/l); commercial sodium TPP pentahydrate 2.1 g/l (see Figure 1); pH adjusted at room temperature with NaOH.

**Reagent grade $Na_5P_3O_{10} \cdot 5H_2O$ was used

***Synthesis method described by Quimby (1950) and Zhou & Carnali (2000)

All samples were then dry heated at 95 °C (samples labeled "dry95°C") or/and heated at 95 °C in contact with a detergency solution for one week (samples labeled "wet95°C"), before the characterization of the solid by XRD, ATR-IR, and in the case of sample SE5 also by ^{31}P MAS-NMR. The synthetic samples were compared to the real precipitates obtained during washing machine cycles.

Real washing machine incrustations were synthetized in Reckitt & Benckiser Laboratories in Mira (VE, Italy). 24 cycles, each cycle lasting one hour, were performed with a European-type washing machine, i.e. with an internal heating system. Detergency solution was renewed for each cycle. Detergency solution was made with 15 liters of tap water adjusted to 43 °F by adding $CaCl_2$ and variable amounts of commercially available domestic detergents: 210 g of Leading Phosphate Detergent 1 (sample RI1); 210 g of Leading Phosphate Detergent 2 (sample RI2); 105 g of Leading Phosphate Detergent 1 plus 88 g of inhibitor 1 (Calgon Water Softener, sample RI3); 105 g of Leading Phospahet Detergent 2 plus 88 g of inhibitor 1 (sample RI4). The samples were collected directly from the surface of the washing machine coil after drying at room temperature at the end of the 24 laundry cycles.

All samples were then dry heated at 95 °C or/and heated in contact with a detergency solution for one

week, before the characterization of the solid by XRD, ATR-IR, and in the case of sample RI1 also by ^{31}P MAS-NMR.

ATR-IR

ATR-IR spectra were collected at the Dipartimento di Chimica IFM, Torino, using a Nicolet 6700 in ATR mode and at the analytical laboratory of Reckitt & Benckiser Italy in Mira (Venezia, Italy) using a Thermo Nicolet 5700. Prior each measurement, the background spectrum was collected to remove any influence of analytical conditions. Each spectrum was collected by using 16 scans with a resolution of 4 cm^{-1}. ATR-IR spectra were processed using the commercial softwares GRAMS 7.01 (Thermo Galactic) and OMNIC 5.2 (Nicolet Instrument Corp.). Characteristic frequencies were determined by second derivative with derivation interval of 18 cm^{-1}.

XRD

Diffraction patterns were collected at the Department of Chemistry "G. Ciamician" of the University of Bologna (Italy) in the 5-60 °2θ range, using a PANalytical diffractometer with Bragg–Brentano geometry (Cu Kα radiation, detector: X'celerator, step size Δ2θ = 0.0167°, counting time per step = 20 s).

MAS-NMR Measurements Of Solid Precipitates

MAS-NMR measurements were performed at the Department of Materials Science of the University Bicocca of Milan (Italy). ^{31}P spectra were collected at 121.49 MHz or 300.13 MHz respectively for 1H or 31P, with a Bruker Advance 300, operating with a magnetical field of 7.04 T, equipped with a Magic Angle Spinning double resonance probe for solid state with a large internal diameter (4 mm). A spinning frequency of 12.5 KHz was used.

Computer Modelling

For thermodynamic and kinetic modelling purposes the freeware program Phreeqc was used.[8] Phreeqc can model chemical reaction and transport processes in natural and synthetic water solution (speciation, interaction between water solution and solid or gaseous phases, etc.) with a thermodynamic approach

and with the possibility of setting kinetic reactions.

RESULTS AND DISCUSSION

Kinetic Experiments

The typical NMR spectrum of a solution containing all TPP, PYP and ORP species is shown in Figure 2. Similar spectra were collected at different times in order to quantify the speciation kinetics. The peak areas are proportional to the number of corresponding phosphate atoms: molar ratios of phosphate species for each spectrum were thus estimated from the relative peak areas. TPP molar fraction includes all protonated and deprotonated tripolyphosphoric species, and the same holds for PYP and ORP molar fractions. The kinetics of the speciation is monitored by measuring the molar fractions of the species.

Following the Avrami equation:

$y = 1\text{-}\exp(\text{-}kt)^n$ (eq. 3)

where y is the molar fraction of the products (*i.e.* PYP molar fraction plus ORP molar fraction), k is the rate constant (number of transformed moles in time), t is time, and n is a constant related to the mechanism of reaction. After linearizing we obtain:

$\ln \ln [1 / (1 - y)] = n \ln k + n \ln t$ (eq. 4)

so that in the diagram ($\ln \ln [1 / (1 - y)]$) *vs* ($n \ln t$) the data are arranged on a straight lines whose slope is n and crosses the y axis at $n \ln k$. Figure 3 shows all experimental data, while Table 3 reports the results of the linear regressions for all experiments.

Table 3: linear regressions results of kinetic experiments for the TPP hydrolisis. $A = n \ln k$; $B = n$; $\sigma(A)$ is the standard deviation for A; $\sigma(B)$ is the standard deviation for B; R is the linear correlation coefficient.

Label	***A***	**$\sigma(A)$**	***B***	**$\sigma(B)$**	***R***	***n***	**k(mol·min^{-1})**

KE1	-8.03	0.09	1.11	0.01	0.99895	1.11	$7.2 \cdot 10^{-4}$
KE2	-7.77	0.15	1.08	0.02	0.99659	1.08	$7.5 \cdot 10^{-4}$
KE3	-7.66	0.12	1.07	0.02	0.99785	1.07	$7.8 \cdot 10^{-4}$
KE4	-8.01	0.04	1.031	0.004	0.99997	1.031	$4.2 \cdot 10^{-4}$
KE5	-7.79	0.14	1.02	0.02	0.99937	1.02	$4.9 \cdot 10^{-4}$
KE6	-7.89	0.51	0.96	0.06	0.99118	0.96	$2.7 \cdot 10^{-4}$

The resulting values of *n* is close to one, as expected for homogeneous reactions in solution, and the frequency terms *k* for the TPP hydrolisis in solution are in agreement with those reported by Van Wazer et al. (1955) in similar conditions.[5] Indeed it is confirmed that the difference in the hydrolisis rate between pH 9.5 and pH 11.5 is rather small at constant temperature (see experiments KE1, KE2 and KE3). The results show that the hydrolisis rate increases when ionic strenght increases (see KE5 and KE6) and less significantly when initial TPP concentration decreases (see KE4 and KE5). Hydrolysis of PYP to ORP is reported to be one to two order of magnitude slower than hydrolysis of TPP, accordingly our estimation of the *k* value for the hydrolysis of PYP in experiment KE2, which was conducted until complete hydrolysis to ORP occurred, yields $k=7.75 \cdot 10^{-5}$ mol·min^{-1}.

XRD

All precipitates from the precipitation experiments were found to be amorphous to diffraction, similarly to what observed for the real washing machine incrustations. Figure 4 shows a typical XRD pattern of a real incrustation compared to a laboratory synthesis product, no Bragg peaks are observed. Products SE5-dry95°C and RI1-dry95°C were amorphous as well. On the contrary low-crystalline hydroxyapatite was identified in SE5-wet95°C and RI1-wet95°C XRD patterns (Figure 5).

ATR-IR

Crystalline standards were hydroxylapatite [$Ca_5(PO_4)_3OH$] (Hap) for ORP, sodium pyrophosphate decahydrate [$Na_4P_2O_7 \cdot 10H_2O$] (SPYP) for PYP, and anhydrous sodium tripolyphosphate [$Na_5P_3O_{10}$] (STTP) for TPP. Figure 6 shows the reference IR spectra of HAp, SPYP and STTP in the range 800-

1350 cm^{-1}.

Despite the assignments of the bands are not unequivocal, the typical IR features of for the TPP, PYP and ORP anions were tentatively identified. These bands are located in the PO_4^{3-} normal mode ν_3 area between 1000 and 1250 cm^{-1}. Figure 6 clearly shows that a band with wavenumber higher than 1200 cm^{-1} can unequivocally be assigned to TPP, in agreement with Gong (2001).[9] Zhou & Carnali (2000)[10] assigned this band to asymmetric stretching of the central PO_2 group of TPP. Such a frequency was also found in sample SE8 (not shown in figure), which can only contain calcium tripolyphosphate.

On the other hand, when the spectrum shows no absorption features beyond 1200 cm^{-1}, we may exclude the presence of TPP, and the spectrum analysis is focussed on the distinction between PYP and ORP. This is true for all real washing machine incrustations, and thus the IR techniques apparently indicates the absence of TPP in the solid precipitate. We identified two characteristic frequencies: one band around 1090 cm^{-1}, that was assigned to the asymmetric stretching vibration of terminal PO_3, that is present in both PYP and TPP ;[9, 11] another band around 1030 cm^{-1} was assigned to ORP PO_4 asymmetric stretching.[6a]

ATR-IR spectra of our synthetic products are analogous to the incrustation precipitates from the washing cycles (Figure 7).

Zhou & Carnali (2000) also found out that the TPP hydrolisis procedes in the solid phase as long as heat is provided to the system.[10] The measured ATR-IR spectra on samples SE5 and SE5-wet95°C suggest that analogously, the PYP hydrolisis is progressing in the solid precipitate in contact with the solution as long as the detergency solution is heated (Figure 8).

Correlation values between spectra calculated using OMNIC 5.2 show that we cannot distinguish the ATR-IR spectra of a real incrustation from the one of a synthetic product within statistics.

MAS-NMR measurements of solid precipitates

Crystalline standards were hydroxylapatite [$Ca_5(PO_4)_3OH$] for ORP, sodium pyrophosphate decahydrate [$Na_4P_2O_7 \cdot 10H_2O$] for PYP, and anhydrous sodium tripolyphosphate [$Na_5P_3O_{10}$] for TPP;

all standard materials were over 99% pure commercial reagents. Figure 9 shows the MAS-NMR specta of the reference compounds.

We analyzed four samples: sample RI1, sample SE5, sample SE5-wet95°C, and sample SE8 (Figure 10 and 11). Literature data on NMR and MAS-NMR analysis of inorganic (poly)phosphates are relatively scarce. The MAS-NMR data are fundamental to interpret the presence of the phosphatic species in the amorphous materials. Four types of phosphatic species can be discriminated on the basis of Q_n, where n is the number of bridging oxygen atoms with another phosphorous atom: Q_0 are isolated tetrahedra (ORP), Q_1 are chain terminal tetrahedra (PYP and terminal tetrahedra of polyphosphates), Q_2 are chain (polyphosphate) or ring (metaphosphate) tetrahedra, while Q_3 units form 3-D networks (ultraphosphates) that are not involved in the present study. Commonly observed chemical shifts are: Q_0 (2 to 3 ppm); Q_1 (-8 to -6 ppm); Q_2 (-25 to -18 ppm).[12] It should be noted that the chemical shift is also dependent on the cation present: Mcbeath et al. (2006) show that sodium PYP has a chemical shift of -1.93 ppm, whereas this value can be as low as -6.88 ppm for calcium PYP.[13] The shift produces overlapping between the Q_0 peak of ORP and the Q_1 peaks of TPP.

Our interpretation of the measured NMR-MAS spectra is based on the analysis of sample SE5-wet95°C spectrum, showing two peaks at 3.018 and -5.337 ppm: since this sample is constituted by nanocrystalline hydroxyapatite, as confirmed by X-ray diffraction, we assigned the two peaks to Q_0 of ORP (the most intense) and Q_1 of PYP respectively. Comparison of the spectrum of the real incrustations from washing cycles (sample RI1) confirms that the same species are present, although in a different ratio, with a very small quantity of Q_2 (small peak at -20.222 ppm) indicating TPP impurities.

Sample SE5 shows the clear evidence of all the peaks of TPP (see Fig. 11 and Fig12) overimposed on the larger Q_1 peak of PYP at approximately -6.5 ppm. This interpretation is confirmed by the spectrum of sample SE8 (Fig. 12), which shows the same MAS-NMR peaks of sample SE5, and was obtained at room temperature by fast precipitation of Ca-TPP.

This interpretation of the MAS-NMR data indicates that IR spectroscopy cannot discriminate the Q_1

and Q_2 units, i.e. PYP from TPP. Carta et al. (2007a; 2007b) assigned IR bands higher than 1200 cm^{-1} to asymmetric stretching of Q_2 units:[12a, b] thus this vibrational mode must disappear or shift depending on the chemical or crystallographic environment of TPP.

Computer Modelling

Thermodynamic data (association and dissociation constants, solubility products, enthalpy and entropy values) were retrieved from the literature.[6b, 14] The kinetic constants were taken from our experimental results by solution NMR. While it is relatively easy to find thermodynamic constants of aqueous species, values related to solid phases in a system containing $(PO_4^{3-})_{aq}$ - $(P_2O_7^{4-})_{aq}$ - $(P_3O_{10}^{5-})_{aq}$ - $(Ca^{2+})_{aq}$ - $(Mg^{2+})_{aq}$ - $(Na^{+})_{aq}$ are incomplete: there is a wide literature on calcium ORP thermodynamics,[6] but very little attention is dedicated to calcium-PYP and -TPP. Further complications derive from the fact that our solids are amorphous substances that are subjected to variations in composition and in physical properties. Simulations were conducted at 90°C, considering a common detergency solution composition: (Ca/Mg)mol = 2.58; $[CaCl_2 \cdot 2H_2O]$ = 3.1 mmol/l, $[MgSO_4 \cdot 7H_2O]$ = 1.2 mmol/l, Na_2SO_4 = 25 mmol/l, $NaHCO_3$ = 21 mmol; pH 10.50.

The hydrolysis effect on the system is represented in Figure 12. TPP and other anions contribute to calcium and magnesium complexation (Figure 13), decreasing the calcite supersaturation index.

We cannot predict precipitation, because of the lack of thermodynamic data concerning the crystalline phases of PYP (no values of enthalpy of formation are available), and the amorphous phases of PYP and TPP. On the other hand, it is interesting to note how known phosphate phases are more supersaturated than calcite (Figure 14).

This simulation shows the fundamental difference between the real washing machine system and the experimental one in the laboratory: in the former case the detergency solution is replaced with a new one every hour; in the latter case the same solution is heated in the oven for a whole day. The hydrolysis of TPP to PYP and ORP in solution is significant only in this latter case.

We used PHREEQC to simulate laboratory experiments representing homogeneous systems. Real

washing machine systems are characterized by large temperature gradients reaching 100 °C in proximity of the coil. A correct model would need a complete description of the temperature distribution in time and space. Moreover the calculation only takes into account the TPP and PYP hydrolysis in solution, while further transformation occurs in the solid phases.

DISCUSSION AND CONCLUSIONS

Our analysis yielded two different precipitation models, one for the real washing machine (open) system, and another for the laboratory experiments (closed) system.

In the washing machine system the main precipitation agent is $Na_4P_2O_7 \cdot 10H_2O$ that constitutes up to 10 wt% of commercial $Na_5P_3O_{10} \cdot 5H_2O$, so that the solid incrustation on the coil is mainly formed by Ca-PYP, subsequently transforming into ORP. If some TPP is present in the precipitated phase, it hydrolizes as well due to the high temperature of the washing machine coil surface (100 °C).

In the case of the laboratory experiments system, interpretation relies on Figure 1, although unfortunately we don't have an analogous diagram for temperatures higher than 60°C. In any case, at the beginning of the experiment the system lies on the right side of the complexation curve; as the system evolves, TPP hydrolizes and the system moves across the complexation curve: this means that Ca-TPP can precipitate. NMR-MAS spectroscopy clearly shows that the precipitate is mainly constituted by Ca-TPP. Being on the left side of the complexation curve, the calcium TPP precipitation is competitive with calcium PYP. Of course hydrolysis of TPP and PYP to ORP is again possible in the solid precipitate, and the final product is always nanocrystalline hydroxylapatite. Indeed it is known that hydroxylapatite crystallization is inhibited by presence of PYP.[15]

Our results also show that IR spectroscopy cannot discriminate the Q_1 and Q_2 units, i.e. PYP from TPP.

The present work highlights the lack of solubility products and thermodynamic data of the amorphous phases involved in the phosphate systems used in detergency. Although the precipitation of such

materials is largely studied from a phenomenological point of view, it is clear that PYP strongly inhibits hydroxylapatite crystallization, and that hydroxylapatite with controlled crystallinity could be produced by heating starting from amorphous Ca-PYP.

ACKNOWLEDGMENT

The work resulted from a collaboration between the Università di Padova and Reckitt Benckiser Italia s.p.a. through the INSTM consortium. Dr. Angiolina Comotti and Dr. Silvia Bracco kindly helped in the solid-state NMR measurements. Prof. Bruno Longato and Elena Bertacco helped in the liquid NMR measurements.

SUPPORTING INFORMATION

All Figures and relative captions follows.

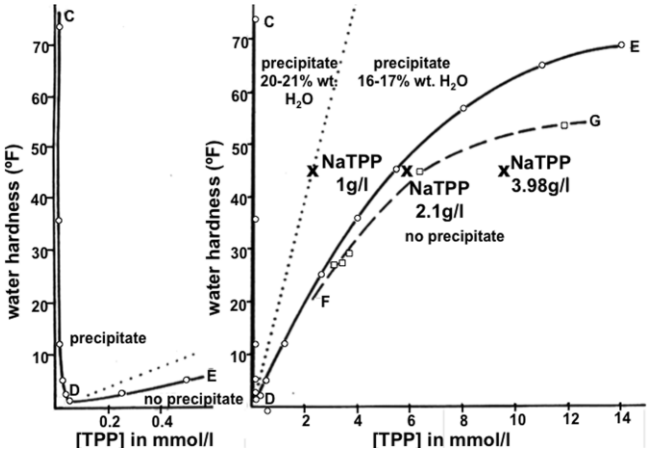

Figure 1: Phase diagram of system $CaCl_2$ – sodium TPP (modified from Quimby, 1954).[2] The area between DE and FG curves is metastable. The simulated detergency solution composition considered for most precipitation experiments in the present work (see experimental part) corresponds to 43°F of

water hardness and 2.1 mmol/l of TPP concentration.

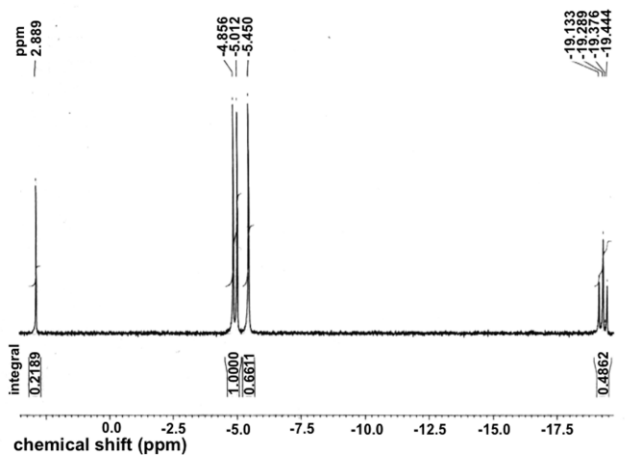

Figure 2 Spectrum of a sample collected from experiment KE1 after 12 h: the central doublet and the triplet at around -20 are assigned respectively to the terminal phousporous and to the central phosphorous of TPP; the central singlet is assigned to PYP, while the ORP one is at the left end of the spectrum.

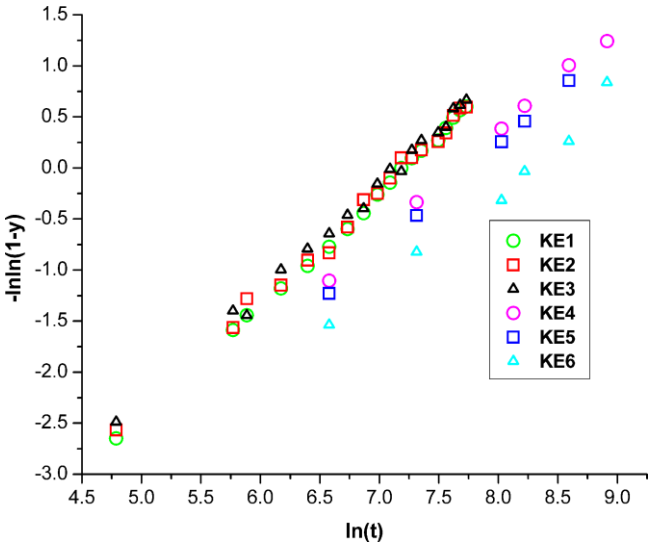

Figure 3: diagram ln ln [1 / (1-*y*)] *vs n* ln *t* of all experimental data.

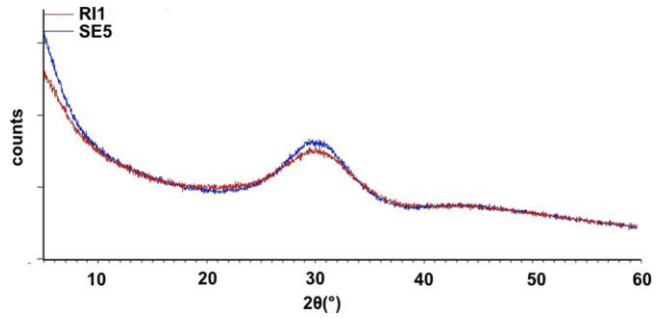

Figure 4: XRD pattern of samples SE5 (blue) and RI1 (red).

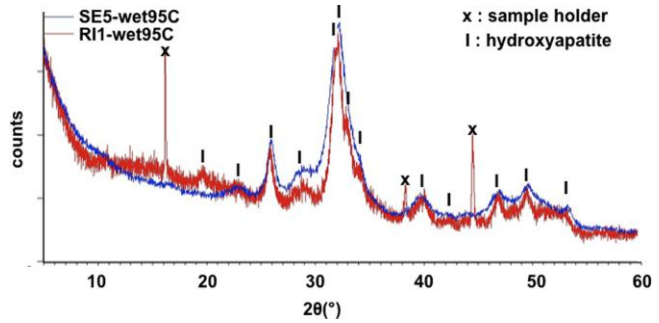

Figure 5: XRD pattern of samples SE5-wet95°C (blue) and RI1-wet95°C (red). Hydroxylapatite peaks are marked with a cross, while sampleholder peaks are marked with a star.

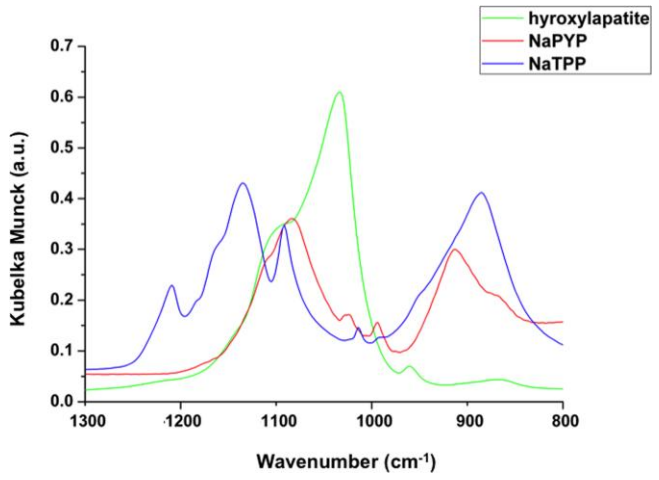

Figure 6: ATR-IR spectra of standards hydroxylapatite (green), sodium PYP decahydrate (red) and sodium TPP (blue).

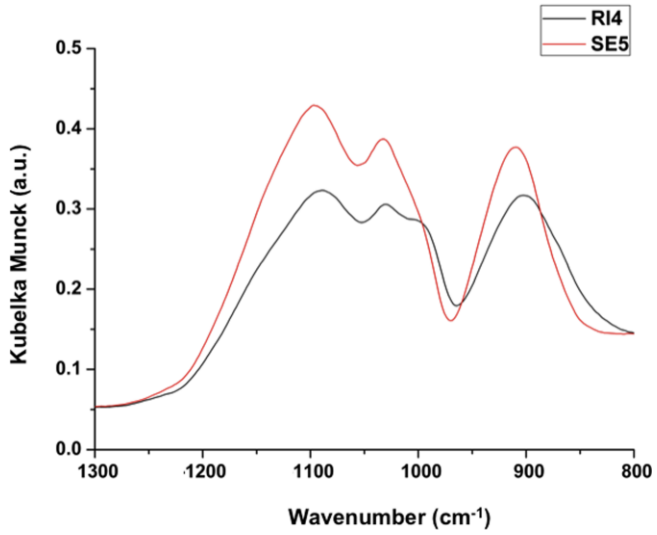

Figure 7: ATR-IR spectra of samples RI1 (black) and SE5 (red).

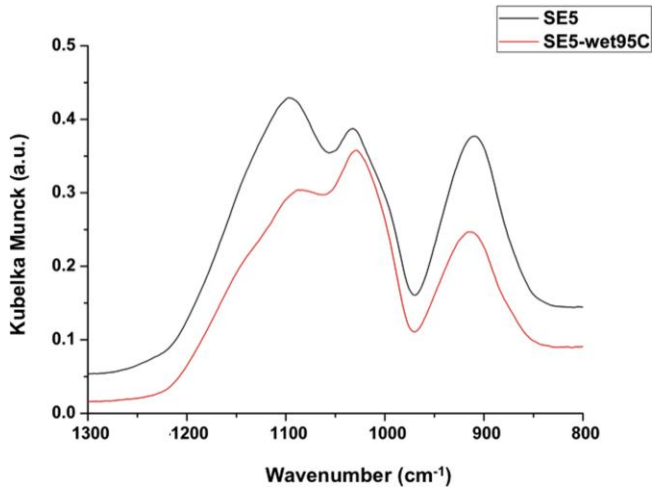

Figure 8: ATR-IR spectra of samples SE5 (black) and SE-wet95°C (red) after one day of heating.

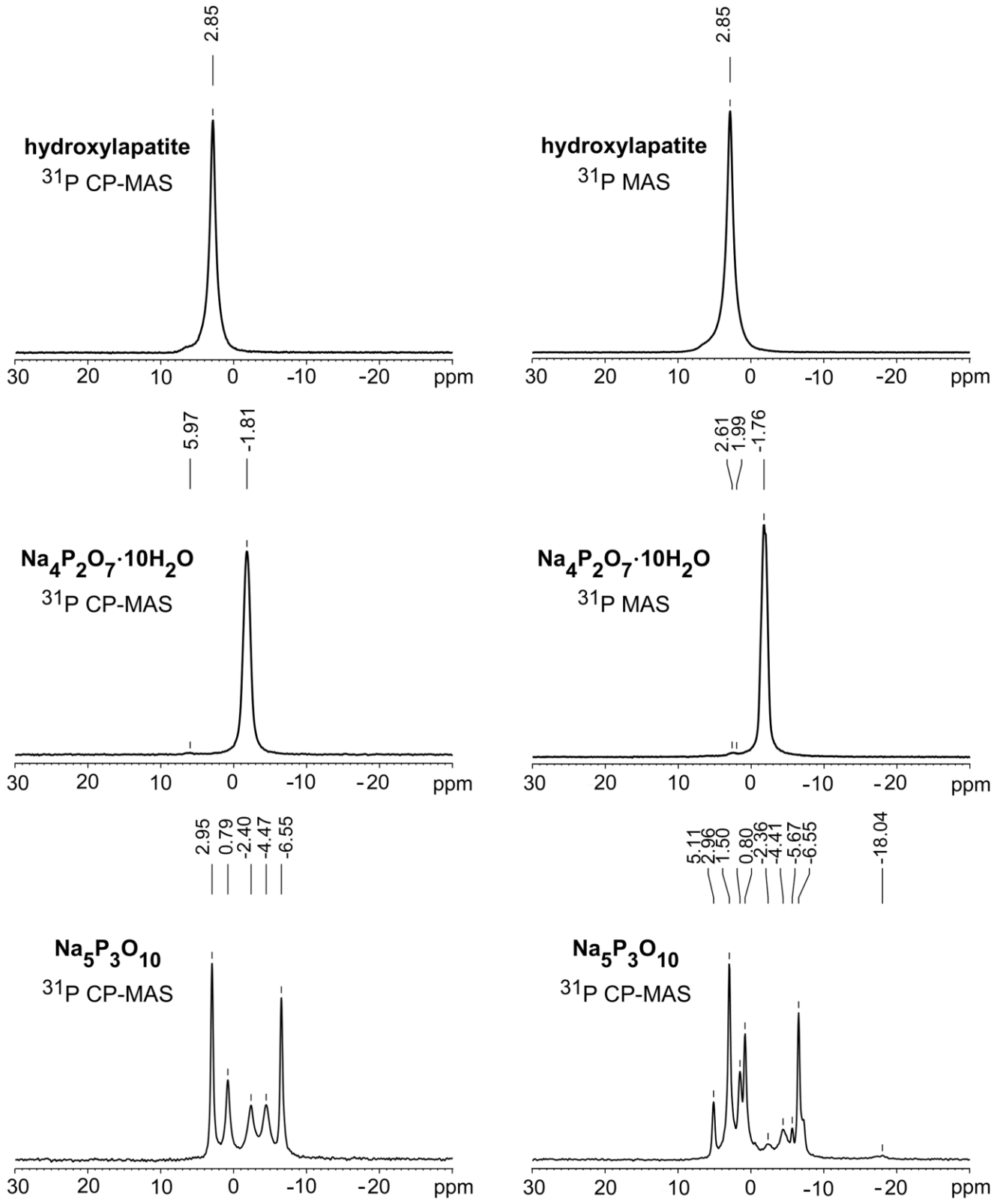

Figure 9: SSNMR spectra (31P CP-MAS on the left and 31P MAS on the right) of standards from top to bottom hydroxylapatite, sodium PYP decahydrate, sodium TPP.

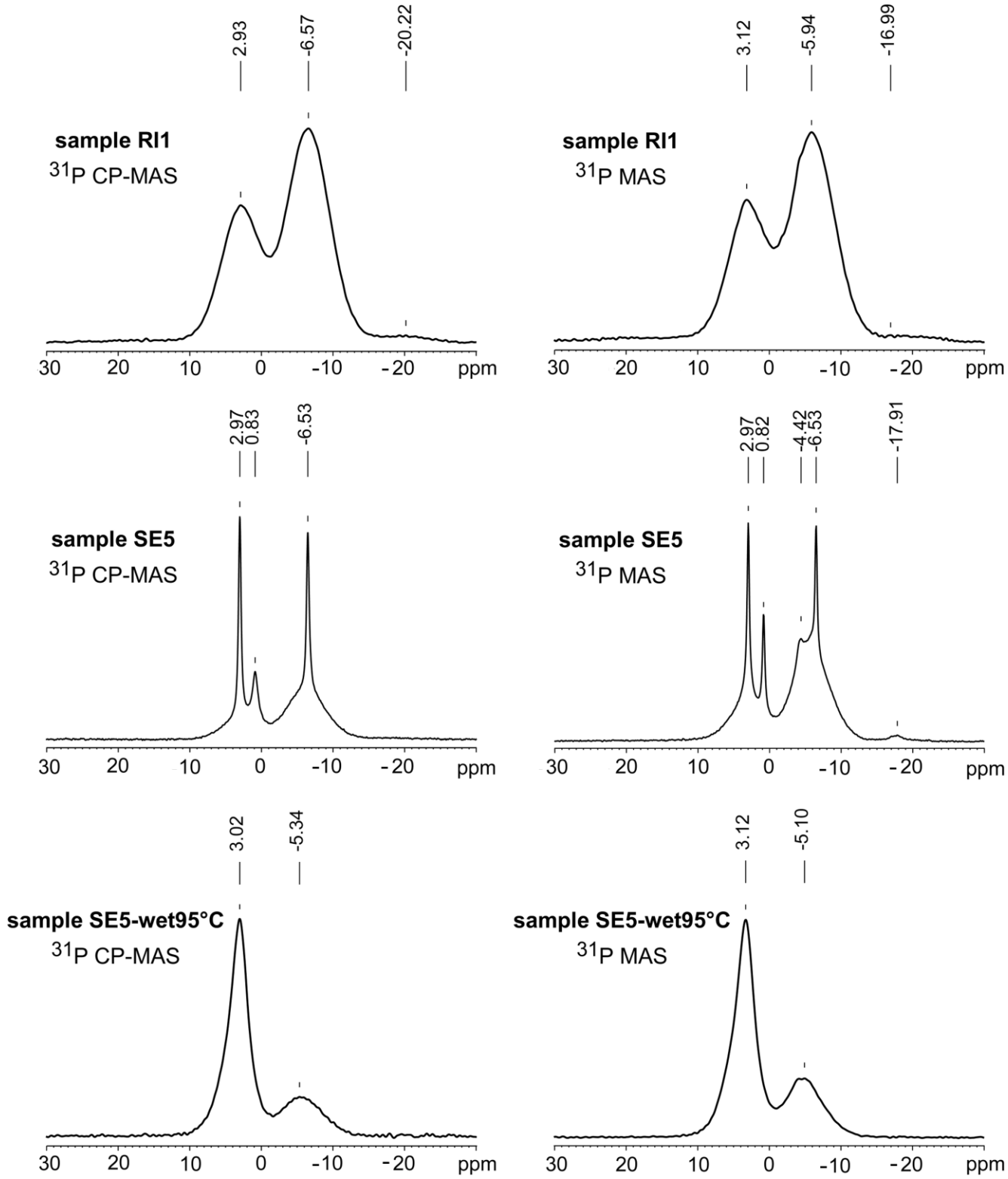

Figure 10: SSNMR spectra (31P CP-MAS on the left and 31P MAS on the right) of samples from top to bottom RI1, SE5 and SE5-wet95°C.

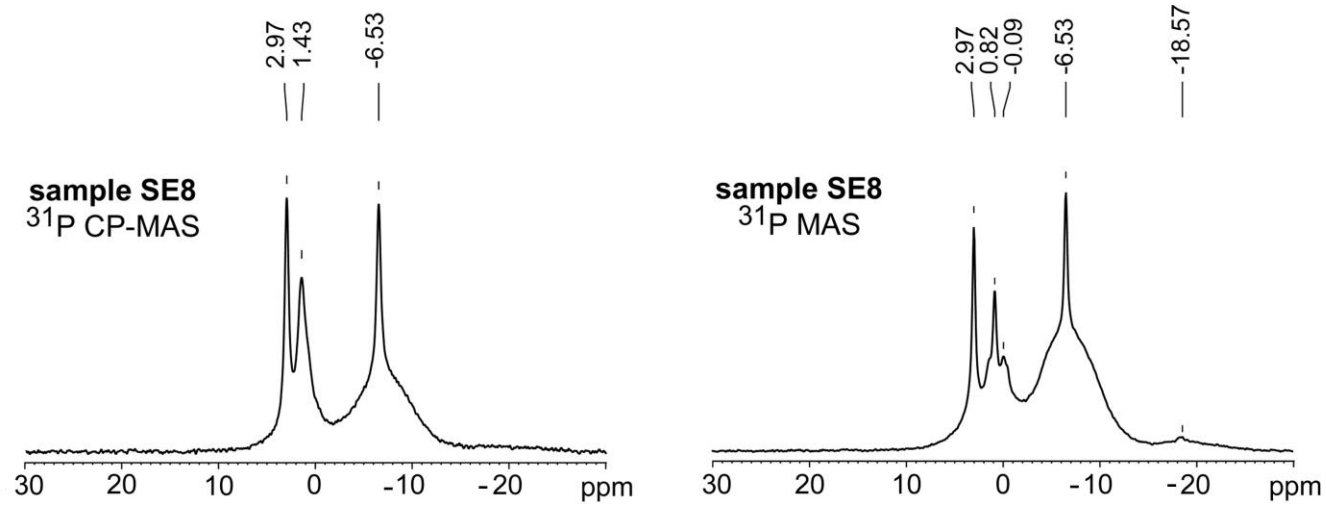

Figure 11: SSNMR spectra (31P CP-MAS on the left and 31P MAS on the right) of sample SE8

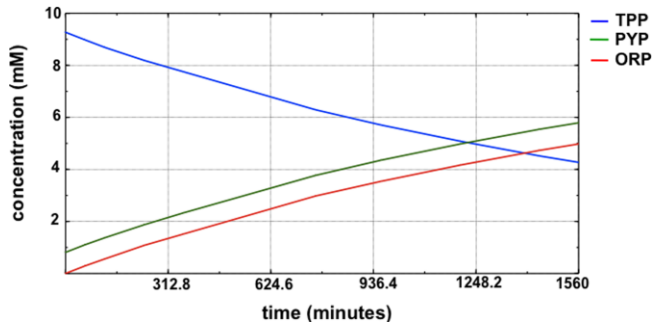

Figure 12: Calculated sum of concentrations of ORP species (red), sum of concentrations of PYP (green) species and sum of concentrations of TPP species (blue) *vs* time for a simulated detergency solution composition at 90°C (see Table 2).

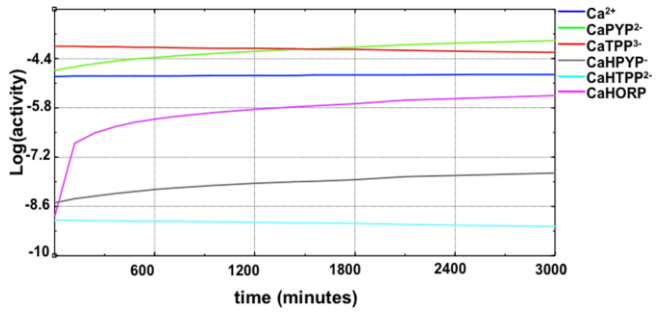

Figure 13: Calculated Log of activity of Ca^{2+} (blue) and of complexes $CaPYP^{2-}$ (green), $CaTPP^{3-}$ (red), $CaHPYP^{-}$ (grey), $CaHTPP^{2-}$ (pale blue), CaHORP (pink) *vs* time for a simulated detergency solution

composition at 90°C.

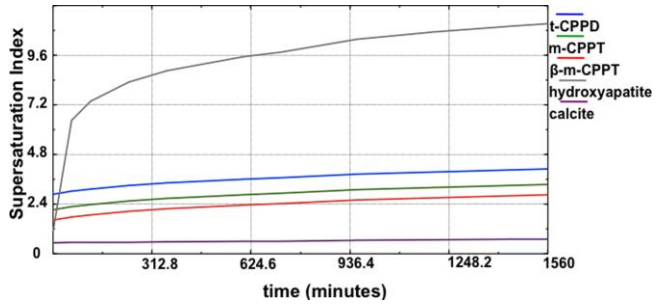

Figure 14: Calculated supersaturation index for triclinic calcium PYP dihydrate (t-CPPD, blue), monoclinic calcium PYP tetrahydrate (m-CPPT, green), *β*-monoclinic calcium PYP tetrahydrate (red), hydroxylapatite (grey) and calcite (purple) *vs* time for a simulated detergency solution composition at 90°C.

REFERENCES

1. Zini, P., *Polymeric additives for high performing detergents*. Technomic Pu. Co.: Lancaster (PA), 1995.

2. Quimby, O. T., *J. Phys. Chem.* **1954,** *58* (8), 603-618.

3. (a) Shen, C. Y.; Dyroff, D. R., *I&EC Product Research and Development* **1966,** *5* (2), 97-100; (b) Shen, C. Y.; Metcalf, J. S., *I&EC Product Research and Development* **1965,** *4* (2), 107-113.

4. Schrödter, K.; Bettermann, G.; Staffel, T.; Wahl, F.; Klein, T.; Hofmann, T., Phosphoric Acid and Phosphates. In *Ullmann's Encyclopedia of Industrial Chemistry*, Wiley-VCH Verlag GmbH & Co. KGaA: 2000.

5. Van Wazer, J. R.; Griffith, E. J.; McCullough, J. F., *J. Am. Chem. Soc.* **1955,** *77* (2), 287-291.

6. (a) Elliott, J. C., *Reviews in Mineralogy and Geochemistry* **2002,** *48* (1), 427-453; (b) Valsami-Jones, E.; Koutsoukos, P. G., Principles of phosphates dissolution and precipitation. In *Phosphorus in environmental technology: principles and applications*, Valsami-Jones, E., Ed. IWA Publishing: 2004; (c) Wang, L.; Nancollas, G. H., *Chemical reviews* **2008,** *108* (11), 4628-4669.

7. Irani, R. R., *J. Phys. Chem.* **1961,** *65* (8), 1463-1465.

8. Parkhurst, D. L.; Appelo, C. A. J., User's guide to Phreeqc (Version 2) - a computer program for speciation, batch-reaction, one dimensional transport, and inverse geochemical calculation. U.S. Geological Survey: 1998.

9. Gong, W., *International Journal of Mineral Processing* **2001,** *63* (3), 147-165.

10. Zhou, Y.; Carnali, J. O., *Langmuir* **2000,** *16* (11), 5159-5168.

11. Michelmore, A.; Gong, W.; Jenkins, P.; Ralston, J., *Physical Chemistry Chemical Physics* **2000,** *2* (13), 2985-2992.

12. (a) Carta, D.; Knowles, J. C.; Smith, M. E.; Newport, R. J., *J. Non-Cryst. Solids* **2007,** *353* (11-12), 1141-1149; (b) Carta, D.; Pickup, D. M.; Knowles, J. C.; Ahmed, I.; Smith, M. E.; Newport, R. J., *J. Non-Cryst. Solids* **2007,** *353* (18-21), 1759-1765; (c) Guerry, P.; Carroll, D. L.; Gunawidajaja, P., N.; Bhattacharya, P.; Carta, D.; Pickup, D. M.; Ahmed, I.; Abouneel, E.; Thomas, P. A.; Knowles, J. C.; Newport, R. J.; Smith, M. E., *Mater. Res. Soc. Symp. Proc.* **2007,** *984*; (d) Kasuga, T., *Acta Biomaterialia* **2005,** *1* (1), 55-64.

13. McBeath, T. M.; Smernik, R. J.; Lombi, E.; McLaughlin, M. J., *Soil Sci. Soc. Am. J.* **2006,** *70* (3), 856-862.

14. (a) Christoffersen, M. R.; Seierby, N.; Zunic, T. B.; Christoffersen, J. r., *J. Cryst. Growth* **1999,**

203 (1-2), 234-243; (b) Irani, R. R.; Callis, C. F., *J. Phys. Chem.* **1960,** *64* (10), 1398-1407.

15. Fleisch, H.; Russell, R.; Bisaz, S.; Termine, J.; Posner, A., *Calcif. Tissue Int.* **1968,** *2* (1), 49-59.